Supplementary Table S1. The clinical characteristics of patients with MPE

Clinical parameters	Patients with MPE (n=50)		
	Lung adenocarcinoma (n=24)	Squamous-cell carcinoma of the lung (n=17)	Small-cell lung carcinoma (n=9)
Sex (Male/Female)	18/6	12/5	6/3
Age ($\bar{x}$ ±SD)	61.2±3.4	65.3± 3.7	63.8± 3.5
Smoking (Yes/No)	15/9	8/9	6/3
Lymph node metastasis (Yes/No)	22/2	17/0	8/1

Supplementary Table S2. The clinical characteristics of patients with NMPE

Clinical parameters	Patients with NMPE (n=50)		
	Pneumonia (n=19)	Tuberculosis (n=17)	Heart failure/ Hypoproteinemia (n=14)
Sex (Male/Female)	8/11	13/4	6/8
Age ($\bar{x}$ ±SD)	57.3±5.2	43.1±9.6	61.6±4.8
Smoking (Yes/No)	7/12	5/12	8/6

Supplementary Table S3. The phenotype analysis of CD163+CD14+ cells and cytological analysis of 20 cases with MPE

Patients No.	CD163+CD14+ cells (%)	Cytological analysis (first time)	Cytological analysis (second time)	Cytological analysis (third time)
1	6.3	−	−	+
2	12.1	−	+	
3	3.9	−	−	+
4	16.7	−	−	+
5	21.0	−	−	+
6	10.1	−	−	+
7	26.0	−	+	
8	15.6	−	−	+
9	8.3	−	−	+
10	11.1	−	−	+
11	6.9	−	−	+
12	5.2	−	−	+
13	19.2	−	−	+
14	15.8	−	−	+
15	12.2	−	−	+
16	8.9	−	−	+
17	6.4	−	−	+
18	5.3	−	−	+
19	28.5	−	+	
20	22.7	−	+	

Supplementary Figure S1

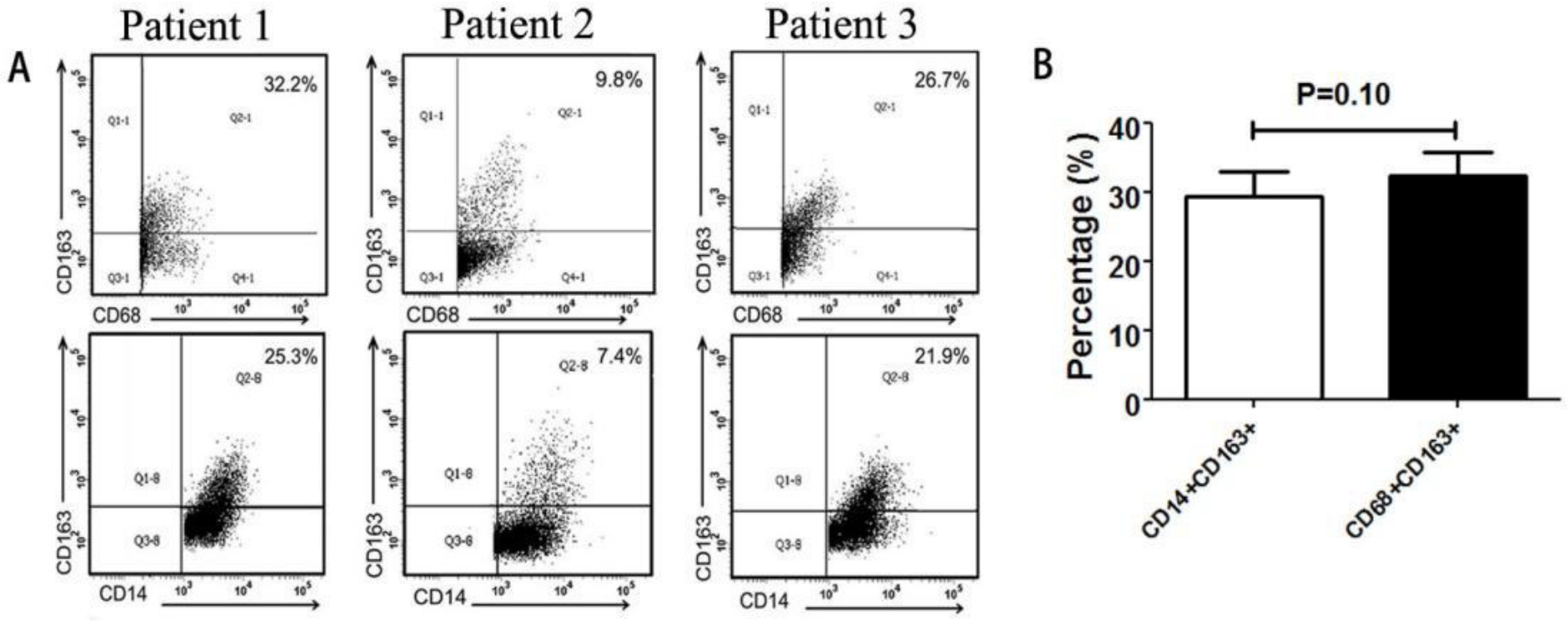

Supplementary Figure S1. Comparison of phenotype analysis of CD68+CD163+ and CD14+CD163+ cells in MPE (n = 30).

A, CD163, CD68 and CD14 were labeled on mononuclear cells in MPE. The cell population in the dot plots was gated on CD68+ or CD14+ cells. Three representative analyses are shown. **B**, Comparison of CD68+CD163+ and CD14+CD163+ cell frequency in MPE . Results are presented as a scatter diagram.

Supplementary Figure S2

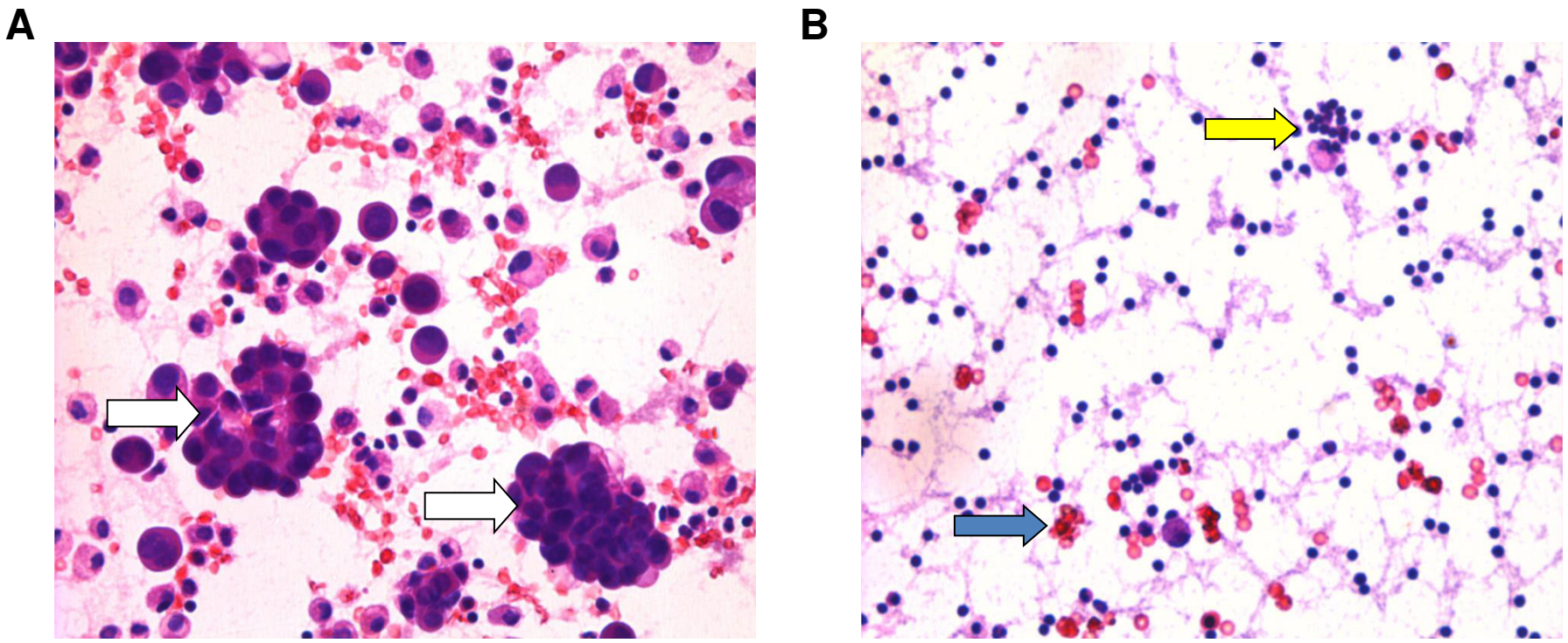

Supplementary Figure S2. Cytological analysis of MPE and NMPE.
A, Red blood cells, lymphocytes, and adenocarcinoma cells with deep-stained large nuclei (white arrow) were visualized in pleural effusion from a lung cancer patient by using sedimentation smear microscopy (×400). One representative analysis is shown. **B**, More red blood cells (blue arrow), lymphocytes (yellow arrow) and a few mesothelial cells were visualized in inflammatory pleural effusion by using microscopy (×400). One representative analysis is shown.

Supplementary Figure S3

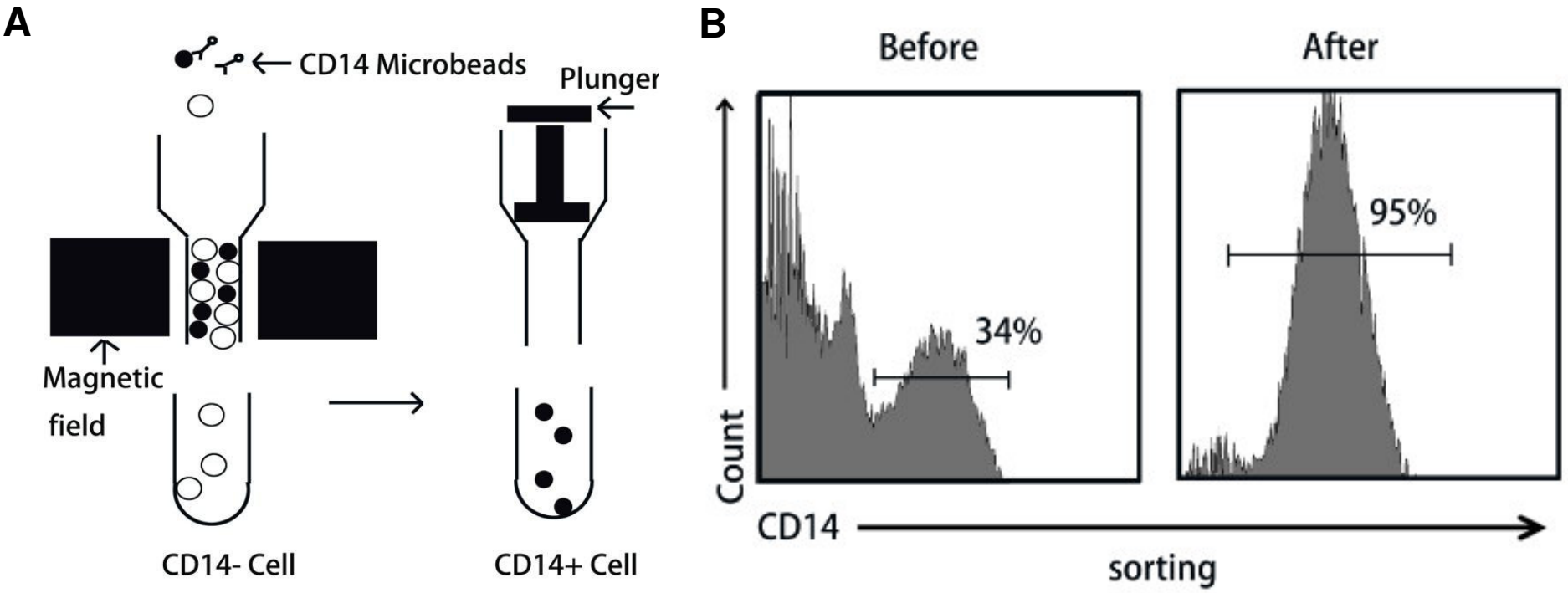

Supplementary Figure S3. CD14+ monocytes were purified using MACS.
A, CD14+ cells were sorted from pleural effusion-derived mononuclear cells by using MACS. The sorting procedure is depicted in the diagram. **B**, CD14 was labeled on these purified and non-purified cells. The purities of CD14+ cells were analyzed before and after sorting by flow cytometry.

Supplementary Figure S4

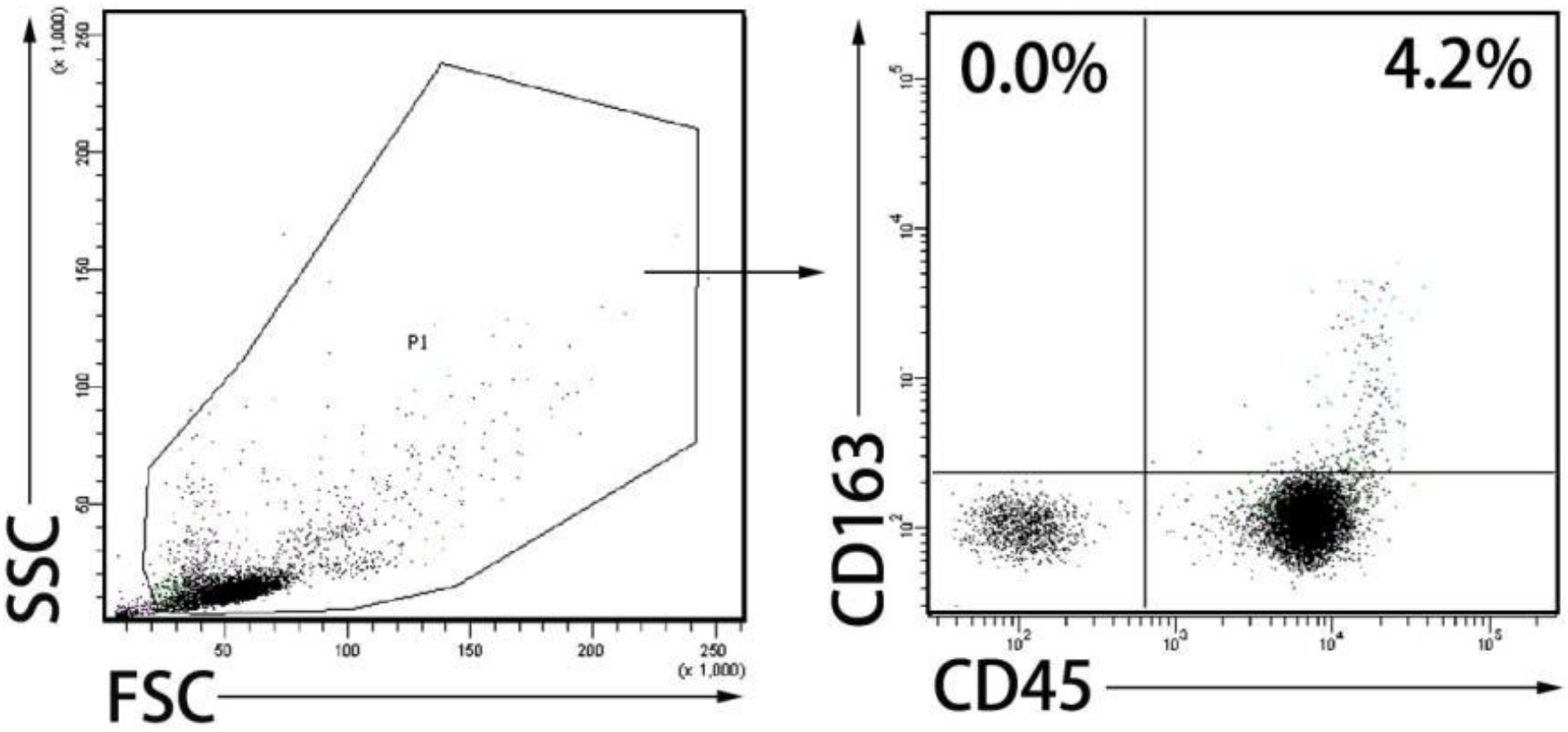

Supplementary Figure S4. Flow cytometry analysis of mononuclear cells with anti-CD45 and anti-CD163 antibodies labeling.
Mononuclear cells from pleural effusion or peripheral blood were stained with human anti-CD45 and anti-CD163 antibodies. One representative analysis is shown.

Supplementary Figure S5

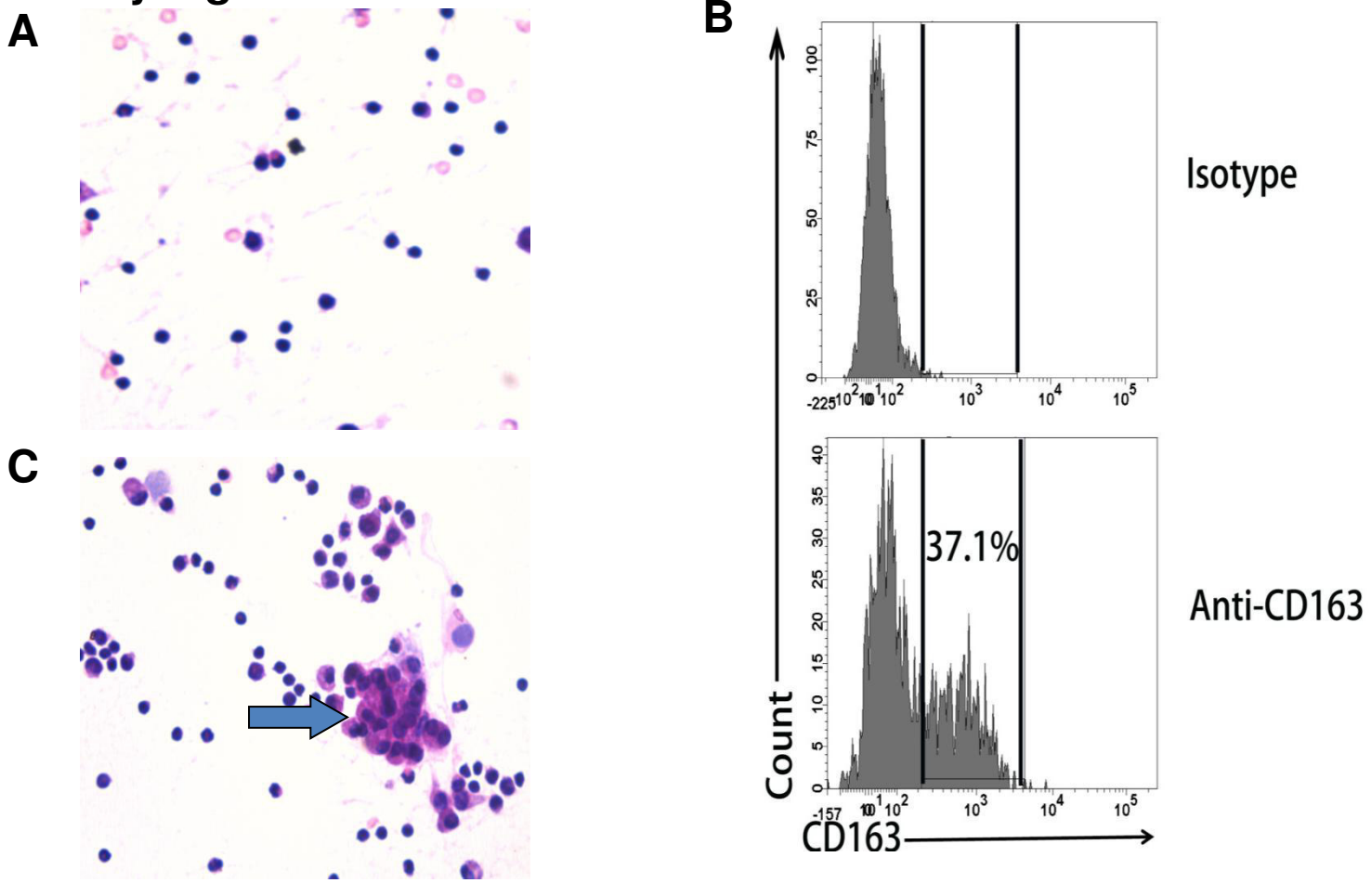

Supplementary Figure S5. High percentage of CD163+CD14+ cells in pleural effusion confirmed to be MPE by tumor cytology.

A, Tumor cells were primarily not detected in pleural effusion by tumor cytology. One representative analysis is shown. Only lymphocytes and mesothelial cells were observed by microscopy (×400). **B**, CD163+ cell frequency was analyzed by flow cytometry. **C**, Presence of tumor cells with deep-stained large nuclei (arrow) in pleural effusion from the same patient was ultimately confirmed by cytological analysis (×400).